

Keller, J. C. Hensel, and F. Stern, CONF-700801 (U. S. AEC Division of Technical Information, Springfield, Va., 1970), p. 422.

<sup>30</sup>D. E. Aspnes, Phys. Rev. Lett. **28**, 168 (1972).

<sup>31</sup>D. S. Kyser and V. Rehn, Bull. Amer. Phys. Soc. **16**, 373 (1971).

<sup>32</sup>D. E. Aspnes, Phys. Rev. **153**, 972 (1967).

<sup>33</sup>The small polarization dependence of the fundamental

direct edge in Ge reported by Fischer (Ref. 24) results from exceeding the low-field limit, and does not occur at higher thresholds where the lifetime broadening is much larger.

<sup>34</sup>This simple picture, which neglects hybridization, Coulomb effects, degeneracy, etc., has been found to give quite accurate polarization dependences for lower energy thresholds in GaAs and InP. See Ref. 28.

## Extreme Ultraviolet Transmission of Crystalline and Amorphous Silicon\*

Frederick C. Brown and Om P. Rustgi

*Department of Physics and Materials Research Laboratory, University of Illinois, Urbana, Illinois 61801*

(Received 6 December 1971)

High-resolution  $L_{III,II}$  absorption spectra are presented for well-characterized films of amorphous and crystalline silicon. The crystalline spectrum shows features which are related to the detailed conduction-band structure of silicon. These features are not seen for the amorphous material presumably because of the lack of long-range order. The amorphous spectrum rises less steeply than the crystalline and has a broad peak near threshold.

Much attention has recently been given to the comparison of electronic-state densities in amorphous and crystalline solids.<sup>1,2</sup> In this paper we present very high-resolution absorption spectra near the  $L_{III}$  edge (photon energy 99.8 eV) of both amorphous and crystalline silicon. The observed spectrum for crystalline silicon is such that band-density maxima, and even one or two critical points, can be identified upon comparison with band theory. The spectrum of the amorphous material is dramatically different in that the peaks and critical structure associated with the band details are not seen.

Transmission measurements on thin films of silicon were carried out using the synchrotron continuum from the 240-MeV electron storage ring at the University of Wisconsin Physical Science Laboratory.<sup>3</sup> Earlier results were reported on both evaporated layers and a very small etched single crystal of silicon.<sup>4,5</sup> The present results on evaporated films differ, in that both amorphous and crystalline samples of large area have been characterized, and signal to noise has been greatly improved. The 2-m grazing-incidence spectrometer<sup>6</sup> was repositioned so that its Rowland circle was in a plane perpendicular to the orbital plane of the storage ring. A marked increase in counting rate was thus achieved probably mainly as a result of improved polarization ( $\vec{E}$  perpendicular rather than parallel to the plane of incidence) upon reflection

at the focusing mirror and grating. Scans could now be taken at highest resolution (10- $\mu$ m slit-width) with little or no noise so as to reveal minute singularities or changes in slope.

In the present investigation the samples were evaporated in high vacuum ( $10^{-6}$  Torr) using a Varian 6-kW electron gun. The source-to-substrate distance was about 20 cm and the deposition rate 5 Å/sec. The amorphous films were deposited onto NaCl substrates at room temperature, and samples were then floated off on water and picked up on screens. Electron-diffraction analysis of these unbacked films yielded a diffuse ring structure which was used to define a film in the amorphous state.<sup>7</sup>

Crystalline silicon films were prepared by vacuum deposition onto fused silica substrates at an intermediate temperature, less than 500°C, followed by an anneal for several minutes at temperatures up to 1000°C. Recrystallization took place somewhere between 600 and 1000°C depending upon conditions such as film thickness, time of anneal, etc. After floating off on hydrofluoric acid, the unbacked films were analyzed in transmission by electron diffraction. Sharp rings characteristic of the  $\{111\}$ ,  $\{220\}$ ,  $\{311\}$ , and higher-order planes of crystalline silicon occurred.<sup>8</sup> In some cases Bragg spots appeared indicating crystallite size comparable to the focused electron beam. Finally, both amorphous and crystalline film thicknesses (in the range

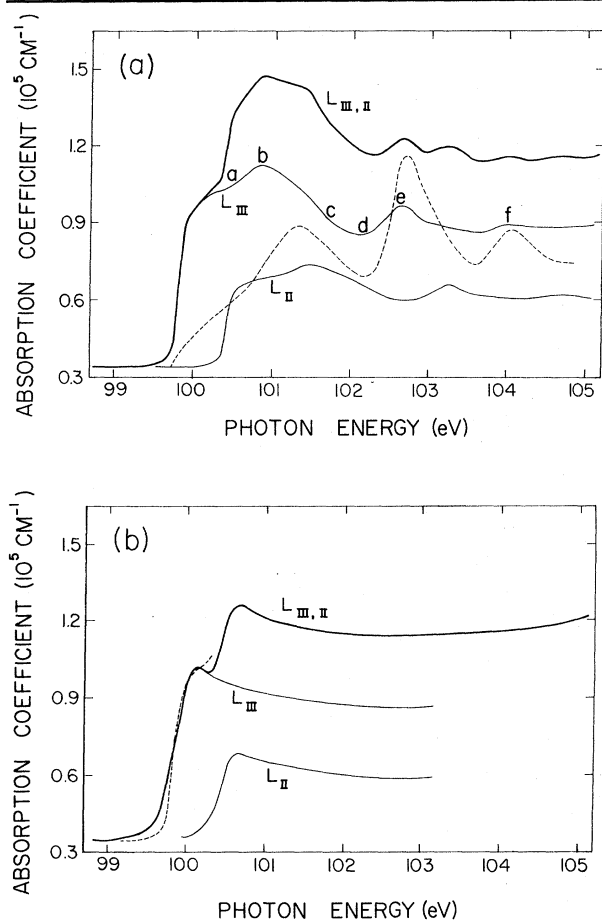


FIG. 1. (a) High-resolution soft-x-ray absorption spectrum of crystalline silicon shown in the uppermost curve. The spectrum is resolved into  $L_{III}$  and  $L_{II}$  components just below this uppermost curve. The dashed line shows the theoretical conduction-band-state density according to Kane, Ref. 12. (b) High resolution absorption spectrum of amorphous silicon. The dashed line is the crystalline spectrum very near threshold as given in (a) above.

1000–2000 Å) were determined with the aid of a quartz-crystal monitor calibrated by the Tolansky technique.

Figure 1(a) shows the observed absorption coefficient (uppermost solid curve) of crystalline silicon on a greatly expanded scale near the  $L_{III,II}$  threshold corresponding to excitation of the  $2p$  inner shell. The random errors in these plots are extremely small, and all details shown are reproducible from scan to scan for different crystalline samples. A spectral bandwidth of 0.05 Å was employed, and the 130-Å krypton lines, known to  $\pm 0.1$  Å, were used for calibration.<sup>9</sup> The absolute coefficients  $\alpha$  in  $\text{cm}^{-1}$  are subject to system-

TABLE I. Observed spectral feature within 4 eV of the absorption edge for crystalline silicon.

Spectral feature	Observed energy (eV)	Energy above threshold (eV)	Tentative assignment
Threshold	$99.84 \pm 0.06$	0	$M_0(\Delta_1) + \text{exc}$
<i>a</i>	100.52	$0.68 \pm 0.05$	$M_0(L_1)$
<i>b</i>	100.87	$1.03 \pm 0.02$	Density max
<i>c</i>	101.69	$1.85 \pm 0.02$	$M_0(\Gamma_{15})$
<i>d</i>	102.17	$2.33 \pm 0.05$	Density min
<i>e</i>	102.67	$2.83 \pm 0.02$	Density max
<i>f</i>	104.02	$3.18 \pm 0.05$	Density max

atic errors, such as enter into stray-light (and thickness) corrections, so that the entire curve might be shifted up or down by perhaps as much as 20%. The observed step height and features near threshold agree with previously published values.<sup>4</sup>

The onset of the  $L_{III}$  absorption (point of maximum slope) occurs at  $99.84 \pm 0.06$  eV, and this is to be compared with a recent very careful  $2p_{3/2}$  binding energy determination from electron spectroscopy for chemical analysis<sup>10</sup> of  $99.6 \pm 0.1$  eV relative to the Fermi level. Comparison of these two numbers would place the Fermi level somewhat above the middle of the band gap. The edge in crystalline silicon, Fig. 1(a), rises with a steepness apparently determined by our instrument resolution. We assume that this threshold corresponds to transitions at, or just below, the  $\Delta_1$  minimum of the silicon band structure.

It can be seen that there are two components to the spectrum of Fig. 1(a) separated by 0.60 eV. This corresponds to the spin-orbit splitting for a hole in the  $2p$  core of silicon.<sup>11</sup> Moreover, the ratio of the initial slopes of the two components is quite close to 2:1 as expected on the basis of statistical weights. With these two bits of information we have decomposed the observed curve into  $L_{III}$  and  $L_{II}$  components as shown in Fig. 1(a). Reproducible spectral features of the  $L_{III}$  curve are labeled and listed in Table I. The dashed curve of Fig. 1(a) is Kane's<sup>12</sup> conduction-band density lined up with the  $L_{III}$  threshold and with ordinate normalized in order to approximate the  $L_{III}$  spectrum well above threshold. Note the very good agreement between theory and experiment as regards the positions of maxima and minima. Auger scattering can occur 1.1 eV above threshold, and presumably this is why the higher band density peaks are broadened in the

observed spectrum. Although the upper maxima coincide remarkably well, the maximum  $b$  occurs about 0.4 eV lower than the first density peak of theory. Perhaps this is reasonable considering difficulties in determining the exact potential<sup>13</sup> and the sensitivity of the critical points in this region. The new experimental values in Table I are useful in deciding between the results of different band theories.<sup>14</sup>

Notice that the initial rise and threshold in Fig. 1(a) are greatly enhanced compared to the band density before peak  $b$ . Most transitions from the core to states widely distributed throughout the Brillouin zone are dipole allowed. The assumption of constant average matrix elements, which we have used in our considerations, is probably not the most important factor.<sup>15</sup> We believe that the threshold is enhanced as a result of the Coulomb potential of the core hole. Exciton lines are not resolved because of small binding energy due to dielectric screening in the solid. This is in contrast to silicon core spectra in a gas where deep excitation states can be resolved.<sup>16</sup> It would be well to have a good optical-response theory for the solid where the photon generates an electron-hole pair formed between the inner shell and band states near the  $\Delta_1$  minimum.

Figure 1(b) shows the observed  $L_{III,II}$  spectrum for an amorphous silicon film. This spectrum was taken with the same resolution as Fig. 1(a). Although the threshold occurs in almost exactly the same place for both types of material, the other crystal features listed in Table I are absent in the amorphous case. This must be because of the breakdown of long-range order. Note that in Fig. 1(b) a kind of peak occurs near threshold which is not seen in Fig. 1(a). This might be because of increased localization of the electron-hole pair in the amorphous case, but also it could be a density-of-states effect. The Penn-Phillips model yields a peak near the conduction-band minimum, as recently discussed by Thorpe and Weaire.<sup>1</sup>

The  $L_{III}$  threshold of amorphous silicon is noticeably less steep than for the crystalline material [compare with the dashed curve, Fig. 1(b)]. By unfolding the instrument bandwidth, assumed Gaussian, we estimate that the amorphous threshold extends about 0.15 eV below that of the crystal. It is conceivable that the initial or core levels are broadened by a varying potential associated with disorder. However, one would not expect this effect to be so large. Another explanation is simply that the amorphous conduction-

band density of states (including electron-hole correction) rises less steeply than the crystalline density. A small foot extends to lower energy as found from recent optical and photoemission studies.<sup>2</sup> It is largely a matter of language whether or not we call this a small tail in density of states. The extra density of states below the crystal band edge must be more or less directly related to the area between the crystalline and amorphous absorption curves at threshold. We cannot reliably estimate the number of these extra states simply by comparison with the theoretical band density shown as a dashed curve in Fig. 1(a), however, because of the probable exciton enhancement at the very edge.

Another approach is to make use of the sum rule<sup>17</sup> leading to an expression for the effective number of electrons  $N_{eff}$  which contribute to the absorption up to energy  $E_1$ , i.e.,

$$N_{eff}(E_1) = (2mV_0/e^2h^2) \int_0^{E_1} E \epsilon_2(E) dE, \quad (1)$$

where  $m$ ,  $e$ , and  $h$  have the usual meanings,  $V_0$  is the atomic volume, and  $\epsilon_2 = nhc\alpha/2\pi E$  with  $n \approx 1.0$  in the extreme ultraviolet. Equation (1) has been applied to the absorption of evaporated silicon over the range 99 to 210 eV.<sup>5</sup> Only about 0.1 electrons per atom contribute to the small part of the spectrum shown in Fig. 1, whereas there are six electrons per atom in the  $L_{III,II}$  core. Assuming that Eq. (1) can be applied on a much finer scale, we find that the extra absorption for the amorphous samples at threshold corresponds to  $5.8 \times 10^{-4}$  electrons per atom or  $2.9 \times 10^{19}$  cm<sup>-3</sup>. The applicability of the above sum rule might be tested by comparing the amorphous and crystalline spectra at higher energies for a loss in area equal to the area under the tail. This probably is the case, but systematic errors in measuring  $\alpha$  for different samples make the comparison very difficult. In any case, we believe that these results nicely illustrate the useful relationship between soft-x-ray response and electronic structure.

The authors would like to express their appreciation to the storing ring staff, especially E. M. Rowe, C. H. Pruett, and R. Otte. Suggestions by Dr. M. Brodsky about film preparation and discussions with Professor C. B. Duke, Professor A. B. Kunz, and Professor W. E. Spicer are much appreciated. The electron diffraction analysis was carefully carried out by Mr. Rick Anderson. Thanks are also due to Mr. W. Scheifley and Mr. J. Slowik in connection with the data reduction.

\*Work supported in part by the U. S. Army Research Office (Durham) under Grant No. DA-31-124-71-G15 and the Advanced Research Projects Agency under Contract No. HC15-67-G-0221.

<sup>1</sup>M. F. Thorpe and D. Weaire, Phys. Rev. Lett. **27**, 1581 (1971).

<sup>2</sup>D. T. Pierce and W. E. Spicer, Phys. Rev. B (to be published).

<sup>3</sup>Supported in part by the U. S. Air Force Office of Scientific Research.

<sup>4</sup>C. Gähwiler and F. C. Brown, in *Proceedings of the Tenth International Conference on the Physics of Semiconductors*, Cambridge, Massachusetts, 1970, edited by S. P. Keller, J. C. Hensel, and F. Stern, CONF-700801 (U. S. AEC Division of Technical Information, Springfield, Va., 1970).

<sup>5</sup>C. Gähwiler and F. C. Brown, Phys. Rev. B **2**, 1918 (1970).

<sup>6</sup>C. Gähwiler, F. C. Brown, and H. Fujita, Rev. Sci. Instrum. **41**, 1275 (1970).

<sup>7</sup>M. H. Brodsky, R. S. Title, K. Weiser, and D. G. Pettit, Phys. Rev. B **1**, 2632 (1970).

<sup>8</sup>S. C. Moss and J. F. Graczyk, Phys. Rev. Lett. **23**, 1167 (1969).

<sup>9</sup>K. Codling and R. P. Madden, Phys. Rev. Lett. **12**, 106 (1964).

<sup>10</sup>A. Melera, Hewlett Packard Corp., Palo Alto, Calif. (private communication). Carbon is used as a reference in the calibration procedure.

<sup>11</sup>F. Herman and S. Skillman, *Atomic Structure Calculations* (Prentice-Hall, Englewood Cliffs, N. J., 1963).

<sup>12</sup>E. O. Kane, Phys. Rev. **146**, 558 (1966).

<sup>13</sup>E. O. Kane, Phys. Rev. B **4**, 1910 (1971).

<sup>14</sup>A. B. Kunz, Phys. Rev. Lett. **27**, 567 (1971).

<sup>15</sup>S. Kirkpatrick, private communication.

<sup>16</sup>W. Hayes, F. C. Brown, and A. B. Kunz, Phys. Rev. Lett. **27**, 774 (1971).

<sup>17</sup>H. R. Philipp and H. Ehrenreich, Phys. Rev. **129**, 1550 (1963).

## Critical Dynamics of SrTiO<sub>3</sub> for $T \geq T_c$

F. Schwabl

*Institut für Festkörperforschung der Kernforschungsanlage Jülich, Jülich, Germany*  
(Received 7 October 1971)

We propose a phenomenological theory for the rotations of the  $BO_6$  octahedra in  $ABO_3$  perovskites at structural transitions. The EPR linewidth behaves as  $\epsilon^{-\nu(1-2\eta)}$  and the ultrasonic attenuation as  $\omega^2 \epsilon^{-\nu(2-\eta)}$  close to  $T_c$ . Further away a crossover to different power laws is predicted. We find an anomaly in the sound velocity.

The perovskite SrTiO<sub>3</sub> undergoes a second-order phase transition at  $T_c = 105^\circ\text{K}$ , below which the TiO<sub>6</sub> octahedra are rotated around one of the cube axes in an alternating way.<sup>1</sup> This and other structural phase transitions of  $ABO_3$  perovskites, where the  $BO_6$  octahedra are rotated around a cube diagonal and axis as in LaAlO<sub>3</sub> at  $806^\circ\text{K}$  and KMnF<sub>3</sub> at  $184^\circ\text{K}$ , have attracted increasing experimental and theoretical interest.<sup>1-5</sup>

In this note we develop a dynamical theory of these transitions based on Mori's theory of Brownian motion,<sup>6</sup> from which the critical behavior of the EPR linewidth is deduced. Then a phenomenological expression for the damping term is proposed to describe the central resonance.<sup>3</sup> We investigate the consequences of this semiphenomenological theory on the dynamic form factor and on the critical anomalies in ultrasonic propagation.

Let us characterize the microscopic angle of rotation of the octahedron at lattice site  $\vec{I}$  around the cube axis  $\alpha$  by  $\varphi_{\vec{I}}^\alpha(t)$  and introduce the staggered angles

$$\hat{\varphi}_{\vec{q}}^{\alpha} = \sum_{\vec{I}} \vec{r} \exp[-i(\vec{q} + \vec{q}_R) \cdot \vec{I}] \varphi_{\vec{I}}^{\alpha}. \quad (1)$$

Here the summation runs over all lattice sites and  $\vec{q}_R = a^{-1}(\pi, \pi, \pi)$  with  $a$  the lattice constant.

Above  $T_c$  the static order-parameter susceptibility for  $\hat{\varphi}_{\vec{q}}^{\alpha}$  is given by

$$\chi^{\alpha\alpha}(\vec{q}, \epsilon) = \chi_0 [\vec{q}^2 - (1 - \Delta)q_\alpha^2 + \kappa^2]^{-1 + \eta/2} \quad (2)$$

for small wave numbers  $\vec{q}$ . The anisotropy term  $-(1 - \Delta)q_\alpha^2$  arises because  $\chi^{\alpha\alpha}(\vec{q}, \epsilon)$  depends much less on the component of  $\vec{q}$  which is parallel to the rotation axis, so that  $\Delta$  may be much less than unity. Here  $\kappa$  is the inverse of the critical correlation length  $\kappa = \kappa_0 \epsilon^\nu$  in the conventional notation  $\epsilon = (T - T_c)/T_c$ . We also need to introduce the conjugate momentum  $\hat{P}_{\vec{q}}^{\alpha} = I(d/dt)\hat{\varphi}_{\vec{q}}^{\alpha}$  with the momentum of inertia  $I = M_0 a^2$  given in terms of the oxygen mass.<sup>7</sup>

We start from the microscopic Heisenberg equations of motion for the slowly varying operators  $\hat{\varphi}_{\vec{q}}^{\alpha}$  and  $\hat{P}_{\vec{q}}^{\alpha}$ . As in the derivation of hydrodynamic equations, the time derivatives of these operators are decomposed into a slowly varying part and into a fluctuating part  $R_{\vec{q}}^{\alpha}$ ,<sup>6,8,9</sup>

$$(d/dt)\hat{\varphi}_{\vec{q}}^{\alpha} = \omega_0^{\alpha}(\vec{q}, \epsilon)\hat{P}_{\vec{q}}^{\alpha}, \quad (3a)$$

$$(d/dt)\hat{P}_{\vec{q}}^{\alpha} = -\omega_0^{\alpha}(\vec{q}, \epsilon)\hat{\varphi}_{\vec{q}}^{\alpha} + R_{\vec{q}}^{\alpha}. \quad (3b)$$